Experimental and Computational Methods for Strength Analyses of Gears

Experimental and Computational Methods for Strength Analyses of Gears

By

Srečko Glodež

Cambridge
Scholars
Publishing

Experimental and Computational Methods for Strength Analyses of Gears

By Srečko Glodež

This book first published 2024

Cambridge Scholars Publishing

Lady Stephenson Library, Newcastle upon Tyne, NE6 2PA, UK

British Library Cataloguing in Publication Data
A catalogue record for this book is available from the British Library

ISBN (10): 1-5275-7562-4
ISBN (13): 978-1-5275-7562-2

TABLE OF CONTENTS

Acknowledgements vii

Foreword ix

Chapter 1 1
Introduction

Chapter 2 23
Strength analyses of gears – Theoretical background

Chapter 3 39
Strength analyses of metal gears

Chapter 4 77
Strength analyses of sintered gears

Chapter 5 93
Strength analyses of polymer gears

ACKNOWLEDGEMENTS

The author wishes to acknowledge gratefully all of his colleagues from the Faculty of Mechanical Engineering, University of Maribor, for their contribution and helpful comments in the framework of different research projects related to gears and gear drives. I am also greatly indebted to all of my students for their inspiration and assistance when solving various problems in the field of gear drives.

Author

FOREWORD

Gears are machine elements used in most engineering applications, mainly in the automotive and aerospace industries. When designing and dimensioning gear drives, the available standardised procedures are usually used for that purpose. The strength analysis (i.e. load carrying capacity) of gears involves the study of the static and fatigue strength (tooth bending strength and surface durability) as well as the scuffing and wear strength, with the purpose of ensuring the predetermined lifetime under the expected operating conditions. Generally, the international standard ISO 6336 is the most frequently used procedure for calculating the load capacity of spur and helical cylindrical gears made of different metallic materials. However, standardised procedures to analyse the load capacity of gears are based on a number of different coefficients that allow for proper consideration of real working conditions (additional internal and external dynamic forces, a contact area of mating gears, gear material, surface roughness, etc.). Furthermore, the standardised procedures are based exclusively on the experimental testing of reference gears, and they consider only the final stage of the fatigue process, i.e. the occurrence of final failure (tooth breakage in a gear tooth root or occurrence of pits on a gear flank). On the other hand, the complete fatigue process leading to fatigue failure may be divided into the following stages: (i) microcrack nucleation, (ii) short crack growth, (iii) long crack growth and (iv) occurrence of final failure. In engineering applications, the first two stages are usually referred to as the *"Crack initiation period",* while long crack growth is referred to as the *"Crack propagation period".* The complete service life of a gear can then be determined from the number of stress cycles N_i required for fatigue crack initiation and the number of stress cycles N_p required for a crack to propagate from the initial to the critical crack length ($N = N_i + N_p$).

When analysing the fatigue behaviour of mating gears, the appropriate computational tool (i.e. Finite Element Method) is often applied to obtain the comprehensive stress/strain field in a gear tooth root or on gear flanks. The computational results are combined with the appropriate fatigue design approach to obtain the fatigue life. The following approaches may be used for that purpose:

- Stress-life approach,
- Strain-life approach,
- Fatigue crack growth approach.

In recent years, sintered gears have been a cost-efficient alternative for machined gears in larger series in the capital goods industry (the automotive industry, electrical appliances, hand-tool industries and other high-volume industrial segments). Due to low prices, low waste, tight tolerances, and evermore improving mechanical properties, Powder Metallurgy (PM) is becoming an interesting alternative mass production process for the future. Significantly, the automotive industry has been using this technology to produce non-vital parts. In general, the international standard ISO 6336 is not suitable for calculating the load capacity of sintered gears. For that reason, alternative computational methods are often used for that purpose, considering all three fatigue design approaches (stress-life approach, strain-life approach, and fatigue crack growth approach). Besides sintered gears, polymer gears are also used widely in many industries and applications, such as office appliances, service and mechatronic devices, household facilities, computer and laboratory equipment, medical instruments, etc. Polymer gears can be produced by classical cutting processes or, for large series production, by injection moulding. Some of the main benefits of polymer gears are high specific mechanical properties, good tribological performance, high resistance against impact loading, ability to absorb and damp vibration, reduced noise, etc. However, polymer gears also have some disadvantages, such as less load-carrying capacity and lower operating temperatures if compared to metal gears, difficulties in achieving high tolerances, relatively high dimensional variations due to temperature and humidity conditions, etc.

This book consists of five chapters. The first chapter introduces the reader to the fundamental magnitudes of gear drives in relation to the cylindrical gear pairs, bevel gear pairs, and worm gear pairs. The second chapter explains the theoretical background of the load capacity of gears, where surface pitting load capacity and tooth root load capacity are described in detail. The third chapter focuses on the strength analyses of metal gears, while chapters four and five describe the strength analyses of sintered gears and polymer gears, including some typical practical examples.

Maribor, January 2024
Author

CHAPTER 1

INTRODUCTION

Gear drives correspond to mechanical drives with the uniform transmission of rotational moving from the driving machine to the driven machine (see Fig. 1.1). Their primary function is to adjust the torque T_1, and rotational speed n_1 of the driving machine (i.e. electromotor, combustion engine, etc.) to the appropriate values T_2 and n_2, which should appear on the driven machine [1.1, 1.2]. Here, the power on the driven side, P_2, is smaller if compared to the power on the driving side, P_1 ($P_2 < P_1$). This is due to losses inside the drive system, which can be expressed by the efficiency of the gear drive $\eta = P_2 / P_1 < 1$.

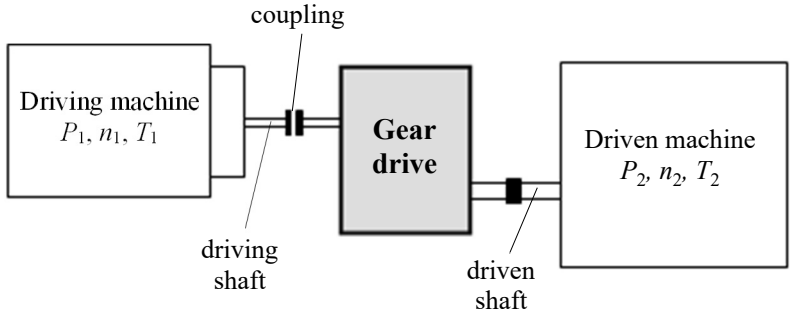

Figure 1.1: The basic principle of the use of gear drive

Gear drives consist of one (one-stage drives) or more (multi-stage drives) gear pairs, which may be differently designed. In general, the following basic gear pairs are most often used in the praxis (see Fig. 1.2):

- *Cylindrical gear pair*: a pair of mating cylindrical gears with parallel axes (Fig. 1.2*a*).
- *Bevel gear pair*: a pair of mating bevel gears with intersecting axes (Fig. 1.2*b*).
- *Worm gear pair*: a pair of mating worm and worm wheel with crossed axes (Fig. 1.2*c*).

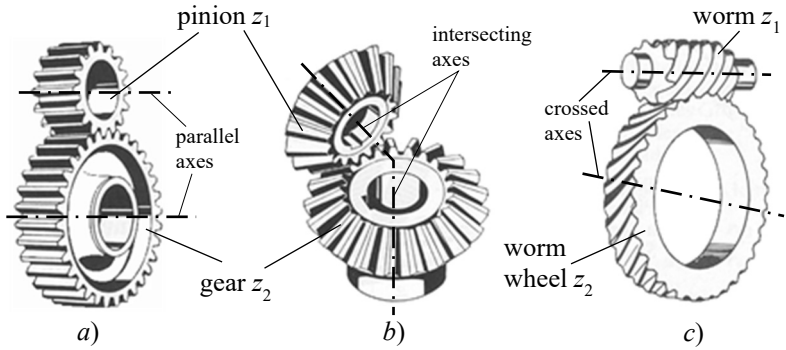

Figure 1.2: The basic designs of gear pairs
a) Cylindrical gear pair, *b*) Bevel gear pair, c) Worm gear pair

The gear pair consists of two gears which are rotating in opposite directions (one clockwise and another counterclockwise). By cylindrical and bevel gear pairs, the smaller gear is called a *pinion,* while the bigger gear is called a *gear*. By worm gear pair, the smaller gear is called a *worm,* while the bigger gear is called a *worm wheel*. The number of teeth is designated as z_1 (for smaller gear) and z_2 (for bigger gear). Table 1.1 shows some typical characteristics of basic designs of gear pairs.

Table 1.1: Typical characteristics of basic designs of gear pairs [1.1]

	Power P_{max} [kW]	Rotational speed n_{max} [min^{-1}]	Circular velocity v_{max} [m/s]	Transmission ratio i_{max}	Efficiency η
Cylindrical gear pairs [1)]	3000	100,000	40 … 100	6 … 8	0.97 … 0.99
Bevel gear pairs [1)]	500	50,000	30 … 80	6 … 10	0.96 … 0.99
Worm gear pairs [1)]	120	40,000	25 … 70	15 … 70	0.40 … 0.96
[1)] The listed maximum values are informative and are valid for one-stage gear drives.					

Cylindrical gears consist of a pair of cylindrical toothed gear wheels and can be designed as spur gears, helical gears, double-helical gears and arrow-shaped gears (Fig 1.3). Furthermore, cylindrical gear pair may be external gear pair, internal gear pair (Fig. 1.4*a*) and rack gear pair (Fig. 1.4*b*).

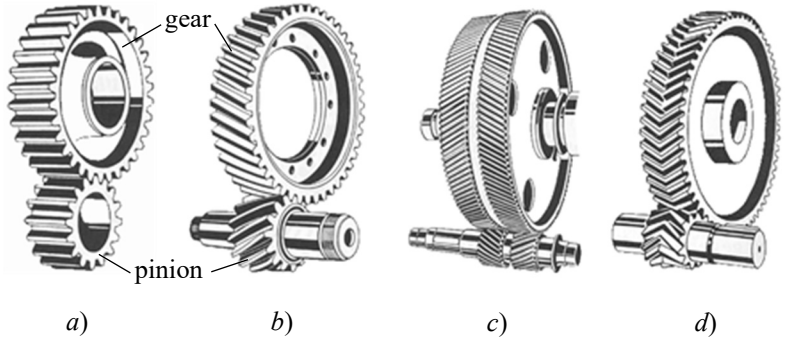

Figure 1.3: Different designs of cylindrical gear pairs
a) Spur gears pair, *b*) Helical gear pair, *c*) Double-helical gear pair, *c*) Arrow-helical gear pair

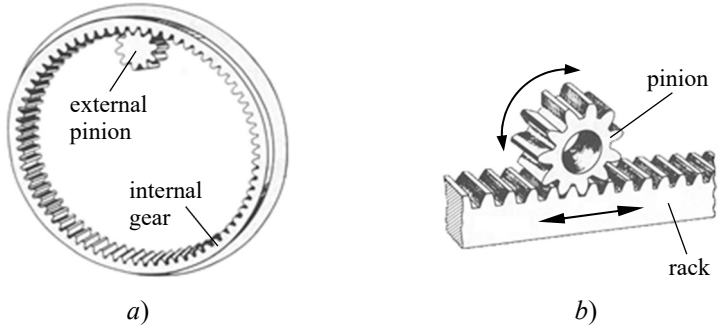

Figure 1.4: Special designs of cylindrical gear pairs
a) Internal cylindrical gear pair, *b*) Rack gear pair

Besides the basic designs of gear pairs, as shown in Fig. 1.2, some special designs of gear pairs are also known in the engineering praxis. *The crossed helical gear pair* (Fig. 1.5*a*) consists of two cylindrical helical gears mounted on the crossed (or skew) shafts. These crossed helical gears are also called screw gears. Unlike the helical gears, which give a line contact between the teeth, a point teeth contact appears in the crossed helical gears. *Hypoid gears* (Fig. 1.5*b*) are spiral bevel gears, the axes of which, however, do not intersect. Hypoid gears are usually used in motor vehicles (cars and trucks), with the axis of the pinion disposed below the crown wheel. *Planetary gear dive* (Fig. 1.5*c*) is a mechanism with gears where one axis (axis of planet gear) is movable around the main axis (axis of sun gear).

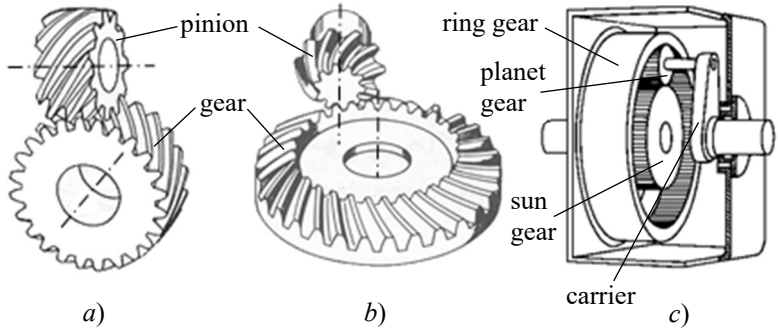

Figure 1.5: Special designs of gear pairs [1.3 – 1.5]
a) Crossed helical gear pair, *b*) Hypoid gear pair, c) Planetary gear drive

1.1 Basic kinematic magnitudes of gear pairs

In this Section, the basic kinematic magnitudes of gear pairs are presented in the case of cylindrical gear pairs. However, the same is also valid for all other gear pairs, as already presented above. In all equations, index "1" is related to the pinion (smaller gear), while index "2" is related to the gear (bigger gear). Fig. 1.6*a* shows the cylindrical gear pair where the pinion z_1 is mating with the gear z_2. Because such a gear pair should transmit the rotational moving from the driving shaft to the driven shaft uniformly, it could be replaced with the rolling of two cylinders with the pitch diameters d_{w1} and d_{w2}. In contact point C (pitch point), the circular velocity of both cylinders should be the same: $v_1 = v_2$.

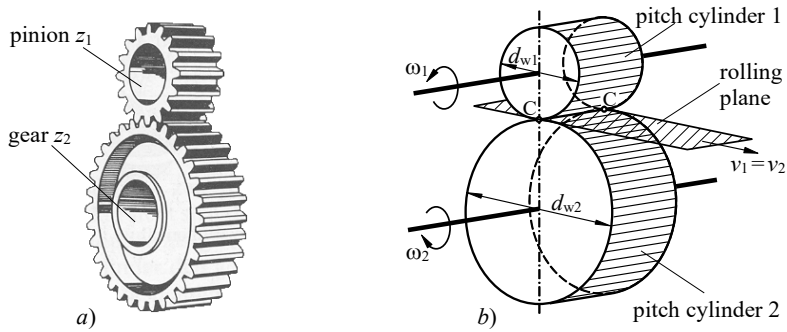

Figure 1.6: Mating of two gears (*a*) and rolling of two cylinders (*b*)

1.1.1 Transmission ratio and gear ratio

The transmission ratio "*i*" of a gear pair is the ratio between the angular velocity "ω" or rotational speed "*n*" of the driving shaft and driven shaft:

$$i = \frac{\omega_{\text{driving}}}{\omega_{\text{driven}}} = \frac{n_{\text{driving}}}{n_{\text{driven}}} \tag{1.1}$$

The gear ratio "*u*" of a gear pair is the ratio between the number of teeth of the gear and that of the pinion:

$$u = \frac{z_2}{z_1} \tag{1.2}$$

It is clear from equations (1.1) and (1.2) that, in the case of the driving pinion, we have $u = i$, while in the case of the driving gear, we have $u = 1/i$.

1.1.2 Main rule of toothing

Figure 1.7 shows the gear pair where the pinion and gear are mating in an arbitrary mating point Y, while the pitch cylinders with diameters d_{w1} in d_{w2} are contacting in pitch point C. The pinion rotates around the axis O_1 with angular velocity ω_1 while the gear rotates around the axis O_2 with angular velocity ω_2. The distances of mating point Y from axis O_1 and O_2 can be designated as $O_1Y = r_{y1}$ for the pinion and $O_2Y = r_{y2}$ for the gear, respectively. The circular velocities in an arbitrary mating point Y ($v_{y1} = r_{y1}\cdot\omega_1$ and $v_{y2} = r_{y2}\cdot\omega_2$) can be distributed in the directions of common normal (v_{ny1} and v_{ny2}) and common tangent (v_{ty1} and v_{ty2}). Since the mating gear flanks must be in contact without backlash and no penetration may appear, the normal velocity components must be equal, i.e. $v_{ny1} = v_{ny2}$. It follows from triangles O_1T_1Y and O_2T_2Y:

$$\begin{aligned} \frac{v_{ny1}}{v_{y1}} = \frac{O_1T_1}{r_{y1}} \quad &\Rightarrow \quad v_{ny1} = \frac{v_{y1}}{r_{y1}} \cdot O_1T_1 = \omega_1 \cdot O_1T_1 \\ \frac{v_{ny2}}{v_{y2}} = \frac{O_2T_2}{r_{y2}} \quad &\Rightarrow \quad v_{ny2} = \frac{v_{y2}}{r_{y2}} \cdot O_2T_2 = \omega_2 \cdot O_2T_2 \end{aligned} \tag{1.3}$$

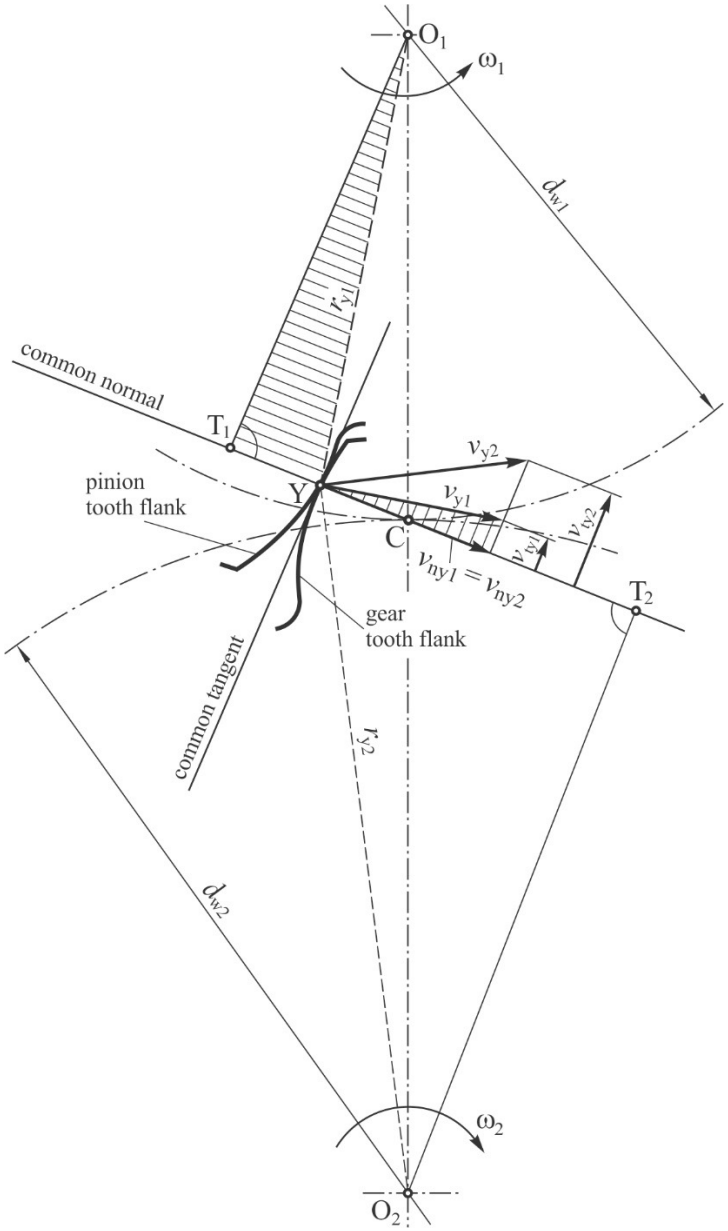

Figure 1.7: Mating of pinion and gear in an arbitrary mating point Y

Considering the condition $v_{ny1} = v_{ny2}$ and the assumption that pinion is a driving part, it follows:

$$\frac{\omega_1}{\omega_2} = \frac{O_2T_2}{O_1T_1} = i \tag{1.4}$$

It is evident from Fig. 1.7 that the common normal intersects the line O_1O_2 in the pitch point C and, therefore, builds the triangles O_1T_1C and O_2T_2C. Considering the relations $O_1C = d_{w1}/2$ and $O_2C = d_{w2}/2$ we get:

$$\frac{O_2T_2}{O_2C} = \frac{O_1T_1}{O_1C} \quad \Rightarrow \quad \frac{O_2T_2}{O_1T_1} = \frac{O_2C}{O_1C} = \frac{d_{w2}}{d_{w1}} = i \tag{1.5}$$

Equations (1.4) and (1.5) define the transmission ratio *i*, which should be a constant value. This requirement is satisfied if two mating profiles (gear flanks) perform a conjugated action. It means that during the rotation of the gear pair, the common normal to the gear flanks at an arbitrary mating point Y must always intersect the pitch point C (see Fig. 1.7). This rule is known as the *main rule of toothing.* Therefore, the gear teeth must be designed so as to get a constant transmission ratio during mating and then to have a conjugate action. Among the possible profiles, involute and cycloid profiles are most often used in the praxis [1.4, 1.6]; see details in Section 1.1.6.

1.1.3 Construction of tooth profile and path of contact

Based on the main rule of toothing, it is possible to obtain the shape of the tooth profile analytically or graphically from the given tooth profile shape of the mating gear, as well as to obtain the path of contact (the line over which the tooth profiles contact during the rolling). Fig. 1.8 shows the construction of the tooth profile of a gear for a given tooth profile of pinion and pitch diameters d_{w1} and d_{w2}. For given points X_1, Y_1 … Z_1 on the tooth flank of a pinion, the appropriate points X_2, Y_2 … Z_2 on the tooth flank of gear can be obtained graphically considering the procedure described below for point X_2. The normal on the tooth flank of the pinion intersects the pitch circle of the pinion at a point X_1'. If the pinion rotates counterclockwise so that point X_1' coincides with pitch point C, point X_1 moves (rotates) to point X. The location of point X can be determined with the intersection of the arc through point X_1 around the axes O_1 and the arc with radius X_1X_1' around pitch point C. Because the normal on the tooth flank of the pinion in point X also goes through pitch point C, point X is, according to the main rule of toothing, the current mating point. At point X, point X_1 on the tooth flank of the pinion comes in contact with point X_2 on the tooth flank of the gear.

Point X_2 in its basic position is obtained with the rotating of the gear back for arc length $X_2'C$. Considering the assumption that pitch circles roll without sliding, the arc lengths $X_1'C$ and $X_2'C$ should be the same. The position of point X_2 is then defined with the intersection of the arc through point X around the axes O_2 and the arc with radius CX around point X_2'. Considering the procedure described above, the other points on the tooth flank of the gear can be obtained. Points X, Y … Z are the current mating points and represent the locations where the tooth flank of the pinion comes in contact with the tooth flank of the gear. The connection line through all mating points X, Y … Z is called *the path of contact*.

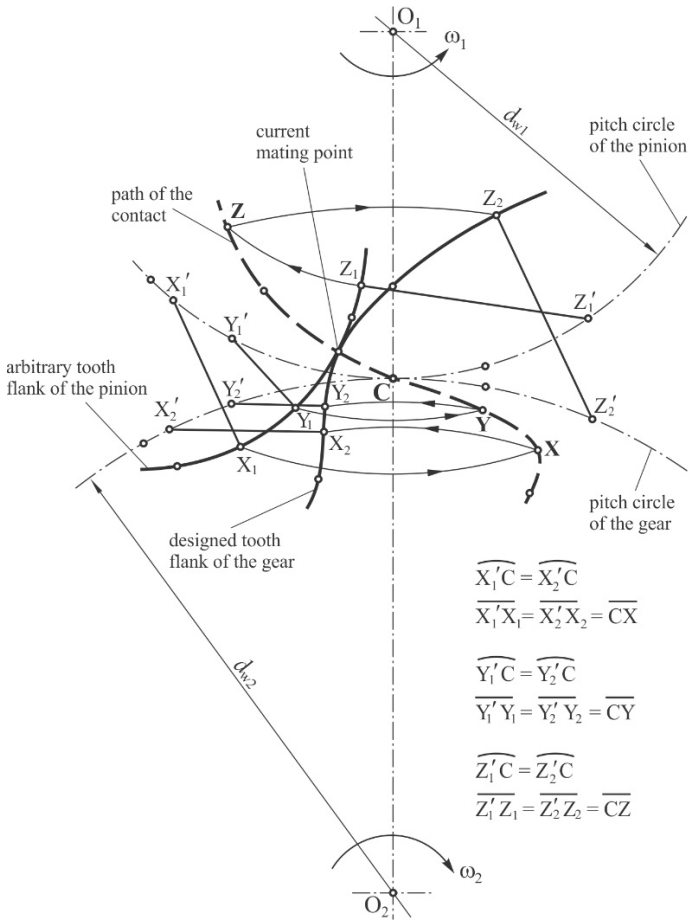

Figure 1.8: Construction of tooth profile and path of contact

Fig. 1.9 shows the mating between pinion and gear in three typical mating points: starting mating point A, pitch point C and ending mating point E. The starting mating point A can be obtained with the intersection of the tip circle of the gear and the path of contact. On the other hand, the ending mating point E can be obtained with the intersection of the tip circle of the pinion and the path of contact. The line AE = g_α represents the length of the path of contact between the pinion and gear during their rotation. It is clear that only active parts of tooth flanks (A_1E_1 for the pinion and A_2E_2 for the gear) mating with each other.

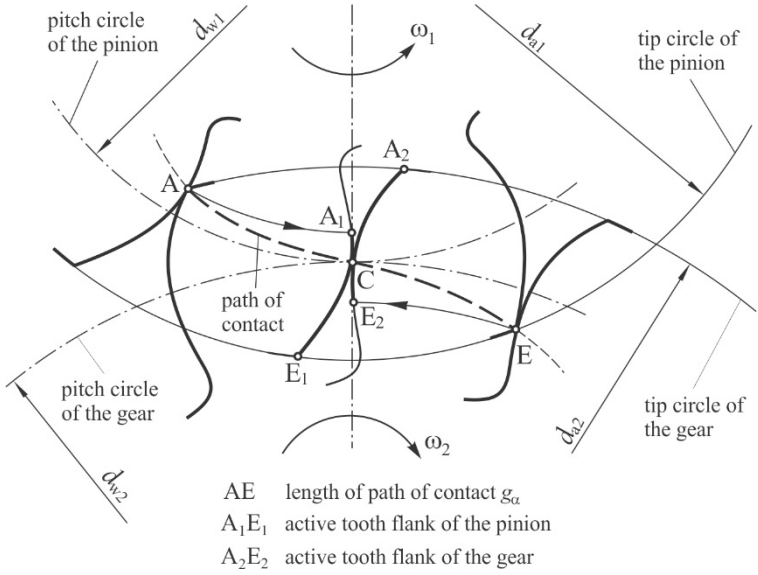

Figure 1.9: Principle determination of the length of the path of contact

1.1.4 Transverse contact ratio

Fig. 1.10*a* shows the mating between pinion and gear in starting mating point A and ending mating point E. The pitch circles of pinion and gear d_{w1} and d_{w2} intersect the belonging gear flanks in points W_1 and W_2 (in starting mating point A) and points W_1' and W_2' (in ending mating point E). Because pitch circles roll on each other without sliding, the arc lengths $g_{p1} = W_1W_1'$ and $g_{p2} = W_2W_2'$ must be the same ($g_{p1} = g_{p2} = g_p$). The mating arcs g_{p1} and g_{p2} represent those parts of pitch circles d_{w1} and d_{w2} at which the pinion mats with the gear.

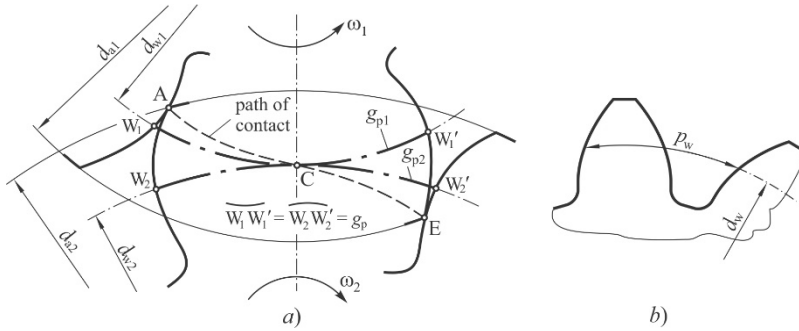

Figure 1.10: Magnitudes for determination of the transverse contact ratio *a*) Mating arc g_p, b) Pitch p_w

Fig. 1.10*b* shows the pitch p_w, which is defined as the arc length between two neighbouring tooth flanks on the pitch circle. For the uniform operation of the gear pair, at least two tooth pairs must always mat, which means that the mating arc g_p must always be greater than pitch p_w ($g_p > p_w$). This can also be expressed with the *transverse contact ratio* ε_α as follows:

$$\varepsilon_\alpha = \frac{g_p}{p_w} > 1 \tag{1.6}$$

1.1.5 Sliding conditions between mating gear flanks

Fig. 1.11*a* shows the sliding conditions in an arbitrary mating point Y before pitch point C. The circular velocities in an arbitrary mating point Y ($v_{y1} = r_{y1}\cdot\omega_1$ and $v_{y2} = r_{y2}\cdot\omega_2$), which are acting perpendicular to the lines O_1Y and O_2Y, can be distributed in the directions of common normal (v_{ny1} and v_{ny2}) and common tangent (v_{ty1} and v_{ty2}). As already described in Section 1.1.2, the normal velocity components must be the same, i.e. $v_{ny1} = v_{ny2}$. Furthermore, the tangential components v_{ty1} and v_{ty2} can be obtained from the triangles O_1T_1Y and O_2T_2Y, and belonging hatched triangles as follows:

$$\frac{v_{ty1}}{v_{y1}} = \frac{\overline{T_1Y}}{r_{y1}} \quad \Rightarrow \quad v_{ty1} = \frac{v_{y1}}{r_{y1}} \cdot \overline{T_1Y} = \omega_1 \cdot \overline{T_1Y}$$

$$\frac{v_{ty2}}{v_{y2}} = \frac{\overline{T_2Y}}{r_{y2}} \quad \Rightarrow \quad v_{ty2} = \frac{v_{y2}}{r_{y2}} \cdot \overline{T_2Y} = \omega_2 \cdot \overline{T_2Y} \tag{1.7}$$

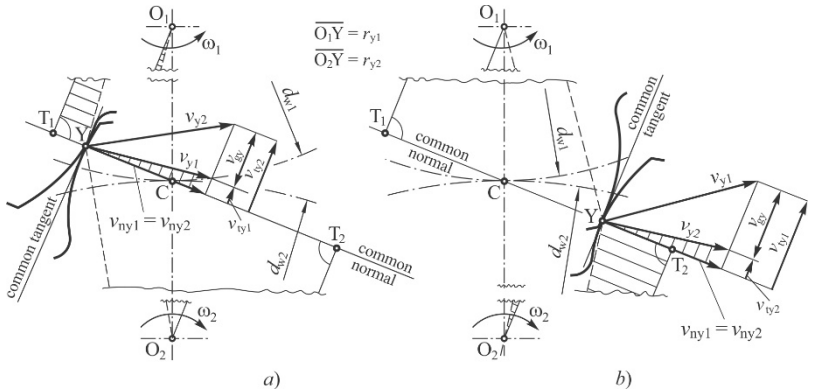

Figure 1.11: Sliding conditions in an arbitrary mating point Y
a) Before pitch point C, b) After pitch point C

The sliding velocities of gear flanks in an arbitrary mating point Y (v_{gy1} for a pinion and v_{gy2} for a gear) are defined as a difference between the tangential velocity components v_{ty1} and v_{ty2}:

$$\begin{aligned} v_{gy1} &= v_{ty1} - v_{ty2} \;=\; \omega_1 \cdot \overline{T_1Y} - \omega_2 \cdot \overline{T_2Y} \\ v_{gy2} &= v_{ty2} - v_{ty1} \;=\; \omega_2 \cdot \overline{T_2Y} - \omega_1 \cdot \overline{T_1Y} \;=\; -v_{gy1} \end{aligned} \tag{1.8}$$

From triangles O_1T_1C and O_2T_2C and with consideration $O_1C = d_{w1}/2$ and $O_2C = d_{w2}/2$, it follows from Fig. 1.11*a*:

$$\frac{\overline{T_1C}}{\overline{O_1C}} = \frac{\overline{T_2C}}{\overline{O_2C}} \quad \Rightarrow \quad \frac{\overline{T_1C}}{\overline{T_2C}} \;=\; \frac{\overline{O_1C}}{\overline{O_2C}} \;=\; \frac{d_{w1}}{d_{w2}} \;=\; \frac{\omega_2}{\omega_1} \tag{1.9}$$

With consideration $T_1C = (T_1Y + YC)$ and $T_2C = (T_2Y - YC)$, it follows from Eqs. (1.8) and (1.9):

$$\begin{aligned} v_{gy1} &= -\,(\omega_1 + \omega_2) \cdot \overline{YC} \\ v_{gy2} &= +\,(\omega_1 + \omega_2) \cdot \overline{YC} \end{aligned} \tag{1.10}$$

Because the sum $(\omega_1 + \omega_2)$ is a constant value, it is clear from. Eq. (1.10) that the sliding velocity v_{gy} only depends on the distance of point Y from the pitch point C. When an arbitrary mating point Y coincides with pitch point C, the sliding velocity equals zero (see also Fig. 1.12).

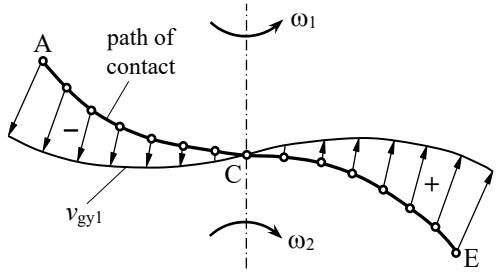

Figure 1.12: Schematic presentation of sliding velocities of pinion along the path of contact

1.1.6 Involute and cycloid profiles of gear flanks

As explained in Section 1.1.2, involute and cycloid profiles are often used in the praxis when designing gear pairs. Both of these profiles correspond to the main rule of toothing and provide uniform rotational moving from the driving to the driven shaft.

Involute gears

Involute of the circle (shorter *involute*), also known as *evolvent of the circle,* is the most often used curve when designing gear flanks. An involute is a path described by any point on a straight line that rolls without sliding on the base circle. The graphical construction of the involute is shown schematically in Fig. 1.13.

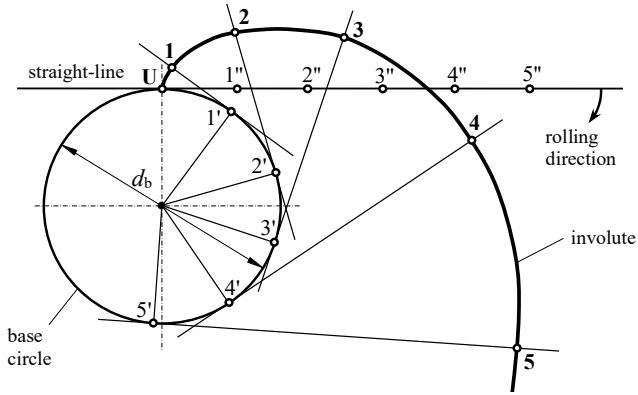

Figure 1.13: Schematic construction of involute of the circle

Fig. 1.14*a* shows the formation of involute tooth flanks schematically. The presented gear pair consists of pinion and gear with fixed centres of rotation O_1 and O_2 and having base circles whose respective diameters are d_{b1} and d_{b2}. T_1 and T_2 are the points of tangency of the straight-line with these base circles. According to the main rule of toothing, the common normale (straight-line) on gear flanks in an arbitrary mating point Y goes through the pitch point C. It is clear that the path of contact is a part of the presented straight-line, which forms the involute profile of both gear flanks. When d_{w1} and d_{w2} represent the diameters of the pitch circles, α is the pressure angle of the toothing with respect to these pitch circles. If such tooth flanks of pinion and gear (involutes 1 and 2 in Fig. 1.14*a*) are limited upwards with tip diameters d_{a1} and d_{a2} and down with root diameters d_{f1} and d_{f2}, the real gear teeth can be obtained (see Fig. 1.14*b*).

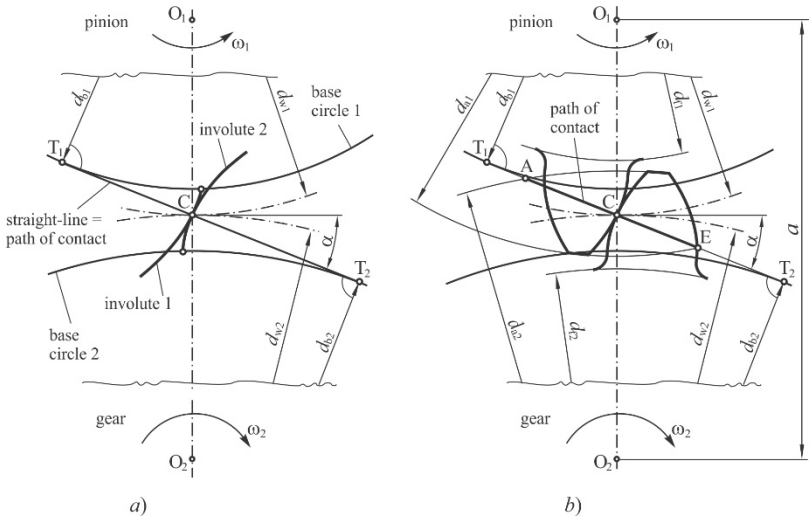

Figure 1.14: Schematic presentation of involute gear pair
a) Formation of involute tooth flanks, b) Formation of pinion and gear tooth

Gears with an involute tooth profile are called *involute* gears and cover approximately 90 % of all globally manufactured gears [1.2]. This is due to the following advantages [1.3]: the conjugate action is independent of the variation of centre distance; it allows to obtain a high accuracy grade of the gears since the standard basic rack teeth have straight-sided profiles (as well as those of the cutting tools derived from them), so they can be made as accurately as possible; a single cutting tool can generate gear wheels of a given module, with any number of teeth.

Cycloid gears

Cycloid of the circle (shorter *cycloid*) is a path described by any point on a rolling circle that rolls without sliding on the base circle (Fig. 1.15). Based on the position of the rolling circle regarding the base circle, three typical cycloids are known: Orthocycloid (Fig. 1.15*a*), Epicycloid (Fig. 1.15*b*) and Hypocycloid (Fig. 1.15*c*).

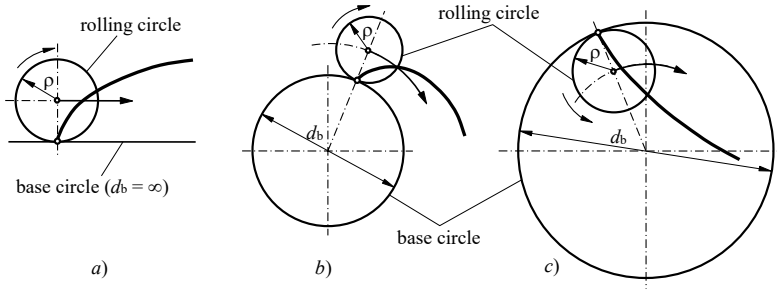

Figure 1.15: Schematic construction of cycloid of the circle
a) Orthocycloid, *b*) Epicycloid, *c*) Hypocycloid

In cycloid toothing, the profile of the tooth flank consists of an epicycloid addendum and a hypocycloid dedendum of the tooth. Fig. 1.16 shows the cycloid gear pair where the pitch circles d_{w1} and d_{w2} coincide with the base circles d_{b1} and d_{b2} ($d_{b1} = d_{w1}$, $d_{b2} = d_{w2}$). According to the main rule of toothing, the common normale in an arbitrary mating point must go through pitch point C, which means that mating gear flanks should have the same rolling circle. Because of the dedendum of pinion mats with the addendum of gear, their flank profiles can be obtained with the rolling of the rolling circle 1 on the pitch circle 1 (hypocycloid 1) and on the pitch circle 2 (epicycloid 2). Similarly, the addendum profile of pinion and dedendum profile of gear can be obtained with the rolling of the rolling circle 2 on the pitch circle 1 (epicycloid 1) and the pitch circle 2 (hypocycloid 2). It is evident from Fig. 16 that the path of contact consists of rolling circle arcs which contact at pitch point C. Under the assumption that the pitch diameters d_{w1} and d_{w2} are known, the shape of tooth flanks of pinion and gear is dependent only on the radii of rolling circles ρ_1 and ρ_2. The best mating conditions (low sliding between mating flanks, satisfy transverse contact ratio) can be obtained considering the following guidelines [1.1]:

$$2\rho_1 \approx 0{,}3 \cdot d_{w1} \text{ or } 2\rho_2 \approx 0{,}3 \cdot d_{w2}. \tag{1.11}$$

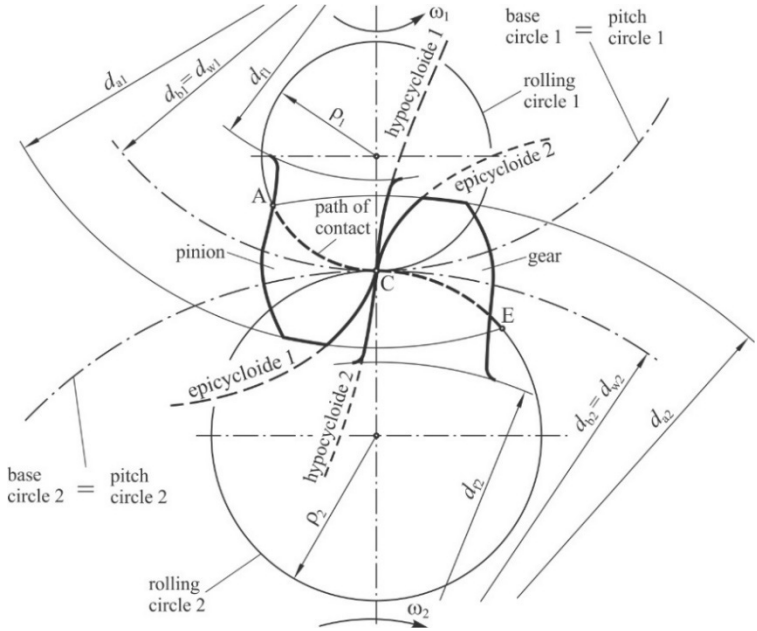

Figure 1.16: Schematic presentation of cycloid gear pair

Cycloide gears have an advantage over involute gears due to lover friction loss and are used primarily on clockwork and similar fine mechanical mechanisms. Furthermore, cycloid gears could be manufactured with a small number of teeth (see examples in Fig. 1.17).

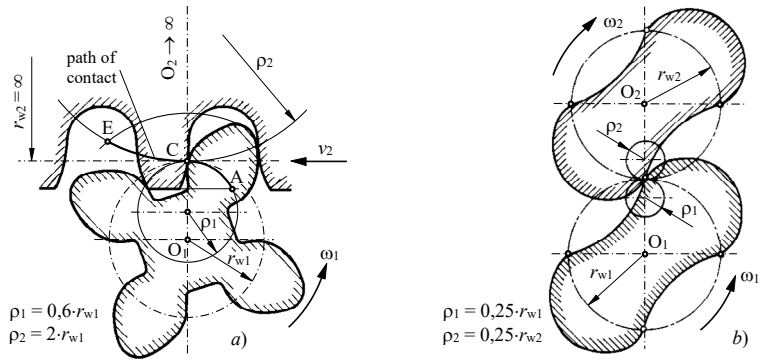

Figure 1.17: Practical examples of cycloid gear pairs [1.4, 1.7]
a) Transformation of rotation to the translation, *b*) Rotors of pump

1.2 Basic magnitudes of involute gears

When describing the basic magnitudes of involute gears [1.8], they are usually related to cylindrical spur gears. However, the cognitions can also be extended to the bevel and worm gears.

Fig. 1.18 shows the basic geometrical magnitudes of the cylindrical spur gear with the number of teeth z. Considering the assumption that the number of teeth z is the whole number and the teeth are distributed uniformly around the reference circle (pitch p is a constant value), the circumference of the reference circle of diameter d can be obtained as follows:

$$\text{circumference} = z \cdot p = \pi \cdot d \quad \Rightarrow \quad \frac{p}{\pi} = \frac{d}{z} = m \tag{1.12}$$

Module m [mm] is the basic magnitude of a gear, which determines the size of the basic rack tooth profile and, thus, the size of the associated gear teeth. Modules are standardised by ISO 54 [1.9]; see Table 1.2. Preferably, the modules from Seriee I should be considered.

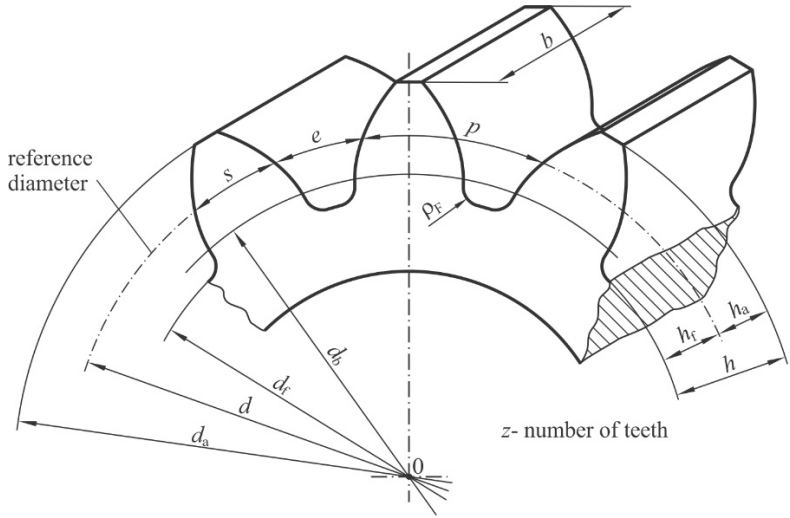

Figure 1.18: Basic magnitudes of cylindrical spur gear

Table 1.2: Standardised modules according to ISO 54 Standard

m [mm] [1]											
I	II	I	II	I	II	I	II	I	II	I	II
1		2		4			7		14		28
	1,125		2,25		4,5	8		16		32	
1,25		2,5		5			9		18		36
	1,375		2,75		5,5	10		20		40	
1,5		3		6			11		22		45
	1,75		3,5		6,5 [2]	12		25		50	

1) Preferably, the modules from Seriee I should be considered.
2) This value can be used only exceptionally.

1.2.1 Involute function

As explained in Section 1.1.6, the involute of the circle is a path described by any point on a straight-line that rolls without sliding on the base circle with radii r_b and centre O (see Fig. 1.19). On the involute, the initial point U and an arbitrary point Y are marked. The rolling straight-line through point Y touches the base circle in point T_Y. The angle between the lines OU and OT_Y is called the *rolling angle of involute* ξ_y, while the angle between the lines OY and OT_Y is the *pressure angle* α_y. The difference between ξ_y and α_y in radians is the *involute function*: $\text{inv}\,\alpha_y = \xi_y - \alpha_y$.

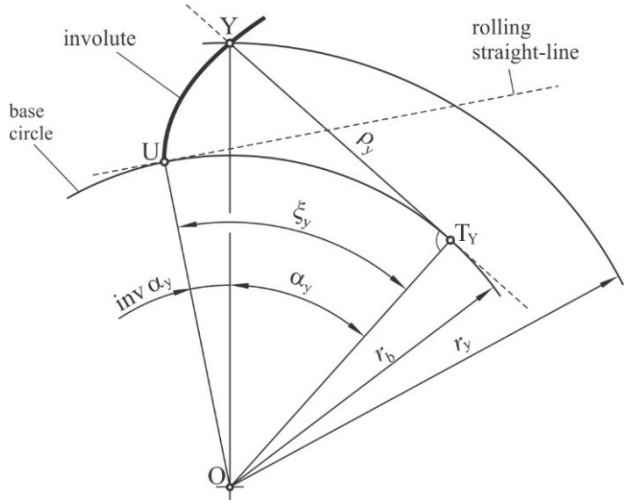

Figure 1.19: Magnitudes for determination of the involute function

It is evident from Fig. 1.19 that the arc length between U and T_Y corresponds to the part of the rolling straight-line between Y and T_Y. Because the arc length between U and T_Y also equals to $r_b \cdot \xi_y$ (ξ_y is given in rad), while the part of the rolling straight-line between Y and T_Y equals to $r_b \cdot \tan\alpha_y$, it follows (the pressure angle α_y should be given in [rad]):

$$\text{inv}\,\alpha_y = \xi_y - \alpha_y \quad = \tan\alpha_y - \alpha_y \tag{1.13}$$

The function invα can be determined by direct computation, considering the pressure angle α as given. Alternatively, a special table available in the scientific literature can be used [1.10]. Determination of the pressure angle α considering invα, as given, is the inverse operation which needs the solution of the non-linear equation: $\tan\alpha - \alpha - \text{inv}\alpha = 0$.

The part of the rolling straight-line between Y and T_Y also represents the curvature radii of involute ρ_y in point Y. It follows from the triangle OYT_Y:

$$\rho_y = r_b \cdot \tan\alpha_y \;=\; \sqrt{r_y{}^2 - r_b{}^2} \tag{1.14}$$

1.2.2 Mating of the involute gear pair

Fig. 1.20 shows the mating of the involute cylindrical gear pair without the profile shift ($x_1 = x_2 = 0$) in pitch point C. In this case, the reference diameters d_1 and d_2 correspond to the pitch diameters d_{w1} and d_{w2} ($d_1 = d_{w1}$ and $d_2 = d_{w2}$). Here, the centre distance can be expressed as $a = (d_{w1} + d_{w2})/2 = (d_1 + d_2)/2$. According to the base definition of the involute function (see Section 1.2.1), the common normale in pitch point C should touch the base circles of pinion and gear d_{b1} and d_{b2} in points T_1 and T_2. Considering the main rule of toothing (see Section 1.1.2), the common normale in an arbitrary mating point should go through pitch point C. Based on these definitions, it can be concluded that, in the case of the involute gear pairs, the path of contact is part of a straight line between the points T_1 and T_2. The length of the path of contact is defined as the length between the starting mating point A and the ending mating point E. As shown in Fig. 1.20, the starting mating point A lies at the intersection between the common normale and gear tip diameter d_{a2}, while the ending mating point E lies at the intersection between the common normale and pinion tip diameter d_{a1}. The angle between the common normale in tangent on the pitch circles is the pressure angle α.

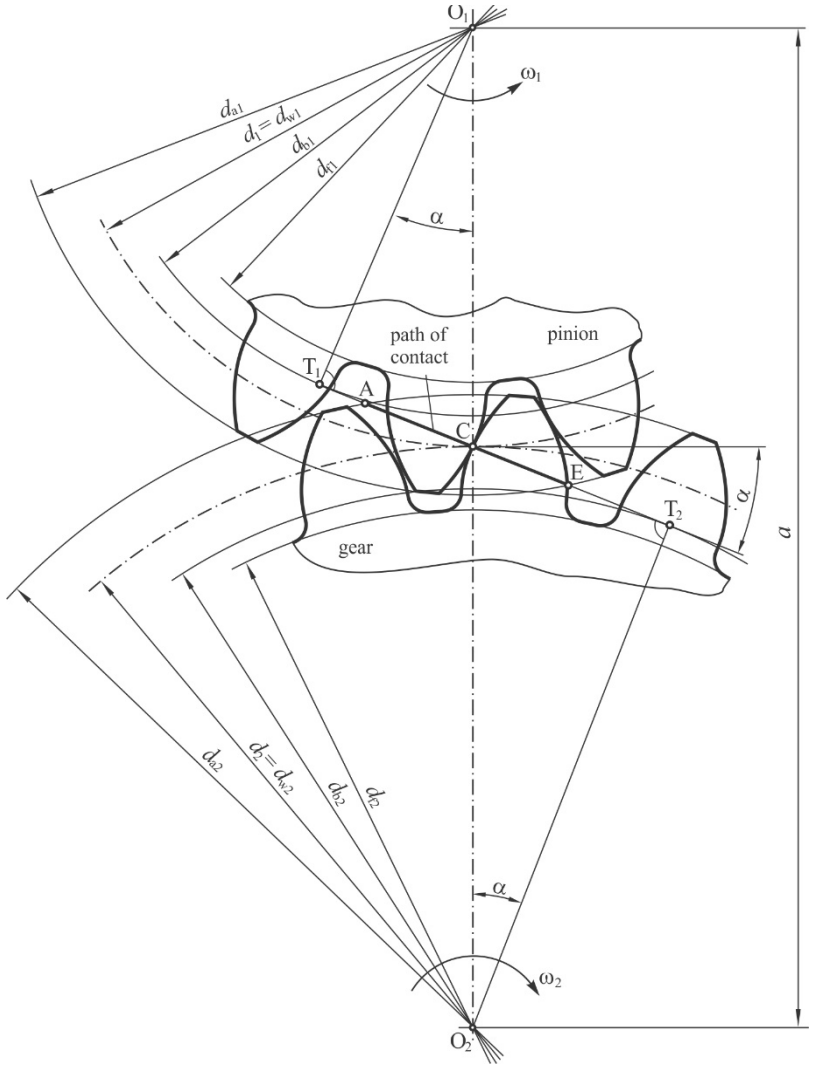

Figure 1.20: Mating of the involute cylindrical gear pair

If the pinion rotates counterclockwise with ω_1, the gear rotates clockwise with ω_2 in accordance with the following equation:

$$\frac{\omega_1}{\omega_2} = \frac{d_{w2}}{d_{w1}} = \frac{d_{b2}}{d_{b1}} \tag{1.15}$$

1.2.3 Standard basic tooth rack

The standard basic tooth rack (Fig. 1.21) defines the characteristics common to all cylindrical gears with tooth profiles having involute geometry. Therefore, each standardised gear wheel may be considered geometrically generated by the standard basic tooth rack with the straight-line profile. This basic rack is a fictitious rack which has, in the section normal to the flanks, the standard basic rack tooth profile, which corresponds to an external gear wheel with a number of teeth $z = \infty$ and reference diameter $d = \infty$.

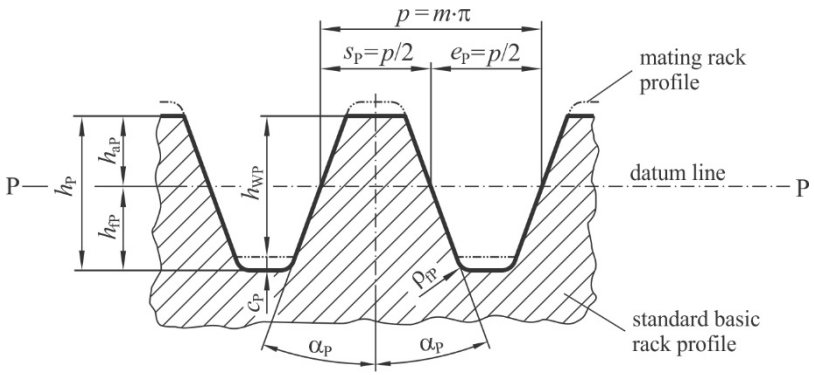

Figure 1.21: Standard basic tooth rack according to ISO 53 [1.11]

The standard basic tooth rack profile refers to a theoretical toothing without backlash. The tooth depth h_P equals $2.25 \cdot m$ (m is the module), while the working portion h_{WP} equals $2 \cdot m$. Addendum h_{aP} and dedendum h_{fP} of this profile equal m and $1.25 \cdot m$, respectively. The working straight portion of the basic rack tooth profile is interconnected with the root line by the fillet, which has the shape of a circular arc with a radius equal to ρ_{fP}. The straight lines of the standard basic tooth rack profile are inclined at the pressure angle $\alpha_P = 20°$ with respect to the axis of symmetry of the tooth. On the datum line, the tooth thickness s_P is equal to the space width e_P, and both are equal to one-half of the pitch p, i.e.: $s_P = e_P = p/2 = \pi \cdot m/2$. The mating rack profile is the rack tooth profile symmetrical to the standard basic rack tooth profile with respect to the datum line P-P, and displaced by half a pitch relative to it. It is evident that the higher the bottom clearance c_P (and then the greater the ratio c_P/m), the larger the fillet radius of the basic rack ρ_{fP}, with the corresponding improvement of the bending strength of the tooth. However, the actual root fillet, which is outside the active profile, can vary depending on various influences such as the profile shift, number of teeth,